Temporal Effects of Neuron-specific Beta-secretase 1 (BACE1) Knock-in on the Mouse Brain Metabolome : Implications for Alzheimer's Disease

Pan, X., & Green, B. D. (2018). Temporal Effects of Neuron-specific Beta-secretase 1 (BACE1) Knock-in on the Mouse Brain Metabolome : Implications for Alzheimer's Disease. *Neuroscience*, 1-15. Advance online publication. https://doi.org/10.1016/j.neuroscience.2018.11.031

Published in:
Neuroscience

Document Version:
Peer reviewed version

Temporal effects of neuron-specific beta-secretase 1 (BACE1) knock-in on the mouse brain metabolome: implications for Alzheimer's disease

Xiaobei Pan[a], Brian D. Green[a*].

[a] Advanced Asset Technology Centre, Institute for Global Food Security, Queen's University Belfast, Belfast, UK.

* Corresponding author

Address: Institute for Global Food Security, Queen's University Belfast, Northern Ireland, UK.

Tel.: +44(0) 2890 97 6541; fax: +44 (0) 28 90976513

E-mail address: b.green@qub.ac.uk

Highlights

- Neuron-specific knockin of human BACE1 age-dependently affects the brain metabolome
- More brain metabolites were significantly altered in 'old' PLB4 mice than 'young'
- Leucine, creatinine, putrescine, various acylcarnitines and phospholipids were affected
- Compared with other AD models (e.g. APP/PS1) fewer metabolites were affected
- Oligomer versus plaque Aβ pathology may have divergent effects on some metabolites

Abstract

Beta secretase 1 (BACE1) is an enzyme involved in the pathogenesis of Alzheimer's disease (AD). PLB4 mice is a neuron-specific human BACE1 knockin mouse model characterised by the accumulation of extracellular Aβ and an AD-like phenotype. In this investigation brain hemispheres from 'young' (4-6 months) and 'old' (8 months) female PLB4 mice and age-matched wild-type littermates underwent targeted LC-MS/MS metabolomic profiling. Powdered lyophilized brain tissue was extracted in ethanol:PBS 85%:15% (v/v)) and a total of 187 metabolites were quantified using a targeted metabolomics methodology. Multivariate statistical analysis produced models that distinguished PLB4 from wild type (WT) mice regardless of their age group. Univariate analysis (t-test) found that more brain metabolites were perturbed in 'old' PLB4 mice than 'young'. Carnosine and 8 phosphatidylcholine species were significantly decreased ($p<0.05$) in 'young' PLB4 mouse brain. In 'old' PLB4 mice a total of 21 metabolites were perturbed including: leucine, creatinine, putrescine and species of acylcarnitines, lysophosphatidylcholines, phosphatidylcholines and sphingomyelin. Within the PLB4 genotype there were a range of age-dependent increases in metabolites. This study indicates that gender-specific responses occur in models of AD-like pathology, but importantly, when changes in PLB4 mice (where Aβ oligomers predominate) are compared with APP/PS1 mice (where Aβ plaques predominate) there are consistent and also divergent effects on the brain metabolome.

Keywords

Alzheimer's disease, metabolites, brain, Beta secretase 1 (BACE1), PLB4.

Abbreviations

aa, diacyl; ae, acyl-alkyl; Aβ, amyloid beta; AD, Alzheimer's disease; APP, amyloid precursor protein; AUC, area under curve; BACE1, Beta secretase 1; CTF, C-terminal fragment; FDR, false discovery rates;

FIA, flow injection analysis; LysoPCs, lysophosphatidylcholines; MRM, multiple reaction monitoring; NFTs, neurofibrillary tangles; OPLS-DA, orthogonal projection to latent structures-discriminant analysis; PCA, principal component analysis; PCs, phosphatidylcholines; PITC, phenylisothiocyanate; PLA2, Phospholipases A2; PS1, presenilin 1; ROC, receiver operating characteristic; SPHs, sphingomyelins; VIP, Variable importance in projection; WT, wild type.

Introduction

Alzheimer's disease (AD) remains the most common form of dementia suspected to cause 60-80% of all dementia cases (Prince et al., 2014). AD is a progressive and fatal neurodegenerative disorder clinically characterised by progressive memory loss, mood changes and cognitive problems. The condition is typified by the pathological accumulation of extracellular amyloid-beta (Aβ) which leads to the formation of amyloid plaques in the brain. It is also known that abnormally phosphorylated tau protein filaments occur in neurons which leads to the formation of neurofibrillary tangles (NFTs) (Blennow et al., 2006; Selkoe, 2004; Skovronsky et al., 2006).

Given the high prevalence and poor prognosis of the disease the development of animal models has become a high research priority. Many of the transgenic models developed are based on the amyloid cascade hypothesis (Elder et al., 2010). They chiefly have involved the insertion or manipulation of mutations in the amyloid precursor protein (APP) and/or the presenilins, both of which are genes causal for familial AD (Elder et al., 2010). Although, transgenic models cannot fully replicate the human disease they have improved our understanding of the pathophysiology of Aβ toxicity, particularly with respect to the effects of different Aβ species and the possible pathogenic role of Aβ oligomers. The APP/PS1 models are important and well established (e.g. APPswe/PS1deltaE9) containing mutations in the gene for APP and presenilin 1 (PS1). Our group have recently performed longitudinal metabolomic profiling of APP/PS1 which revealed that AD-like pathology affects greatly on both the brain and blood metabolomes (Pan et al., 2016).

A recent study described mouse models (PLB4) of AD-like pathology involving the overexpression of BACE1 in the absence of mutant APP expression. The PLB4 mice examined in this study were developed using a targeted knock-in strategy that directed the insertion of the human BACE1 (hBACE1) transgene to the HPRT locus, a permissive site on the X chromosome (Plucinska et al., 2014). BACE1 enzymatically cleaves APP at the N-terminus, generating C-terminal fragments (CTF) which are later cleaved by γ-secretase generating the Aβ peptides (Selkoe, 2001). In PLB4 mice BACE1 activity is only subtly higher (approximately 2-fold higher than endogenous), however, APP processing is clearly shifted toward the amyloidogenic pathway, which results in Aβ accumulation and age-associated behavioural changes consistent with cognitive impairment (Plucinska et al., 2014). Behaviourally, the motor activity of PLB4 transgenic animals is largely intact at 3 months of age but by 6 months it is significantly altered. PLB4 mice displayed deficits in habituation to a novel environment and semantic-like memory (social transmission of food preference) at 3-4 months of age. The cognitive and spatial deficits, such as spatial learning and reference memory (water maze), and spatial working memory (Y-maze), manifested at around 6 months, and were independent from reductions in locomotor activity and anxiety (Plucinska et al., 2014). Complete deletion of BACE1 in APP mutant mice prevents Aβ production, neuron loss and amyloid pathology related cognitive deficits (Laird et al., 2005; Ohno et al., 2007).

Additionally, BACE1 has also been demonstrated to play an important role in glucose metabolism. The BACE1 knock out mouse showed improvement in glucose metabolism, insulin sensitivity and protection from diet-induced obesity (Meakin et al., 2012). The metabolic disturbance was observed in PLB4 mice with increased BACE1 level in the central neuronal system which induced hypothalamic dysregulation, endoplasmic reticulum stress, and Aβ and lipid accumulation (Plucinska et al., 2016).

The aim of this study was to employ a targeted quantitative metabolomic methodology to measure brain metabolite changes occurring in the PLB4 transgenic model. The intention was to

monitor the biochemical responses of the brain to the initial amyloidogenic insult caused by elevated BACE1 activity and understand how this progresses with the neuropathology.

Material and methods

Brain tissue from PLB4 mice

PLB4 mice expressing hBACE1 have recently been described and characterised in detail (Plucińska *et al.* 2014). Homozygous female mice (4-6 months (herein referred to as 'young'): WT: n=8, PLB4: n=7; 8 months (herein referred to as 'old'): WT: n=7, PLB4: n=7) from the University of Aberdeen colony were fasted overnight. Animals were culled and whole brains were rapidly removed and snap frozen in liquid nitrogen, and stored at minus 80°C. Brain hemispheres were transported to Queen's University Belfast on dry ice and stored at minus 80°C prior to processing.

Brain tissue extraction

Mouse brain samples were collected into individual tubes to avoid cross-contamination, then lyophilized and cryogenically milled to a fine dry powder. Powdered post-mortem brain tissue (25 mg ± 0.5 mg) was extracted in 300 µL in a solvent (85% ethanol and 15% PBS buffer) as previously described (Pan *et al.* 2016) using an optimised methodology for brain metabolite profiling (Urban *et al.* 2010). The samples were sonicated (5 min), vortexed (30 sec), centrifuged at (10,000 *g*; 4°C; 5 min) and the supernatant retained for analysis.

Targeted metabolomics

Metabolites in both control and PLB4 mouse brain samples were profiled using the Biocrates AbsoluteIDQ p180 (BIOCRATES, Life Science AG, Innsbruck, Austria), as previously described (Nkuipou-Kenfack et al., 2014; Roemisch-Margl et al., 2012). The samples were analysed on a triple-quadrupole mass spectrometer (Xevo TQ-MS, Waters Corporation, Milford, USA) operating in the multiple reaction monitoring (MRM) mode according to the manufacturer's instructions. The data were recorded in a 96-well format with 7 calibration standards and 3 human EDTA plasma quality control

samples were integrated in the kit. Briefly, 10 µL of brain extract (prepared as described above) was used for targeted metabolomics analysis. Metabolites (amino acids and biogenic amines) were derivatised using phenylisothiocyanate (PITC), followed by separation using a UPLC (I-Class, Waters Corporation, Milford, USA) and quantified using a triple-quadrupole mass spectrometer (Xevo TQ-MS, Waters Corporation, Milford USA) by MRM. The flow injection analysis tandem mass spectrometry (MS/MS) method was used to quantify all the remaining metabolites. Metabolite concentrations were calculated and expressed as µmol/mg tissue.

Statistical analysis

Concentration data for 187 metabolites were appropriately reformatted and exported to Simca 15 (Umetrics, Umea, Sweden) for multivariate analysis. Data were log transformed, pareto-scaled and grouped into PLB4 and WT prior to analysis by principal component analysis (PCA), to identify any potential outliers, and then orthogonal projection to latent structures-discriminant analysis (OPLS-DA). The validity of the model was evaluated based on the residuals (R2X, R2Y) and the model predictive ability parameter (Q2) determined through the default leave-1/7th-out cross validation. The number of components for the OPLS-DA model was optimized using y-table permutation testing (n = 200) and an ANOVA based on the cross-validated predictive residuals (CV-ANOVA) (Eriksson et al., 2008). For CV-ANOVA assessment of significance, a p-value less than 0.05 was considered as significant. Data were then grouped by age and reanalysed by OPLS-DA to highlight significant metabolites explaining the maximum amount of variation between the groups. Univariate analyses consisted of a Student's t-test for metabolites exhibiting a normal distribution or the Wilcoxon Mann-Whitney test for metabolites exhibiting non-normal distributions (Metaboanalyst Version 3.5; (Xia et al., 2015). False discovery rates (FDR, referred to as a q-value) were also calculated using the in-built function in Metaboanalyst in order to account for multiple comparisons. A p-value<0.05 and q<0.8 was considered significant. Receiver operating characteristic (ROC) curves and heat map visualisations were developed for the metabolites short-listed based from the univariate analysis.

Results

Multivariate analysis of metabolomic data

Multivariate analysis was used to build models differentiating all four groups. Figure 1A shows an unsupervised PCA scores plot ($R^2 \leq 0.537$; $Q^2 \leq 0.311$) which moderately separated the groups but with age being a greater discriminating factor than genotype. OPLS-DA model (Figure 1B) made it possible to visibly discern brain samples from young WT, young PLB4, old WT and old PLB4 mice. Using 2 latent and 5 orthogonal components the data produced a discriminant model with a 69 % fit and predictive power of 51 %. To assess the reliability of the OPLS-DA model, we applied CV-ANOVA which gave a p value of 0.047. The model was also validated using a permutation analysis in Simca P v.15 as demonstrated Figure 1C. The principle of this validation is to assess the correlation coefficient of the goodness of fit (R2 and Q2) between the original y-variable and the permuted y-variable while the X-matrix has been kept intact (Eriksson et al., 2006). The results were fitted using a regression line and the Y-axis intercepts of R2 and Q2 were at 0.63 and − 0.42, respectively, which suggest that the OPLS model is valid and does not show over-fit since the regression line of the Q2-points intersect below zero (Eriksson et al., 2006). OPLS-DA was then applied to each age group to assess how accurately models predicted class membership (Q2 cumulative). Models constructed from data from 'young' mice had weak predictive ability of 58%. Models based on data from 'old' mice were only moderately better with the predictive ability of 66%. Variable importance in projection (VIP) plots were created to identify the top 15 metabolites responsible for the observed separation between groups (Table 3).

Metabolites significantly altered by the PLB4 genotype

A total of 9 metabolites (carnosine and 8 PCs) were affected in 'young' mice, and all in all cases these were lower in PLB4 mice (Table 1 and Figure 2). A total of 21 metabolites were affected in 'old' mice (Table 2 and Figure 2). There were 5 metabolites that were lower in PLB4 mice (putrescine, dodecanedioylcarnitine and 3 PCs); and 16 metabolites that were higher in PLB4 mice (leucine, creatinine, 4 acylcarnitines, 5 lysophosphatidylcholines (LysoPCs), 4 PCs and 1 SPH). Only 3

metabolites were commonly affected in both age groups. PC aa C40:1 was reduced 1.46-fold ($p<0.00006$; $q<0.06$) in young PLB4 mice and 1.19-fold ($p<0.03$; $q<0.35$) in old PLB4 mice. PC aa C42:1 was reduced 1.86-fold ($p<0.00009$; $q<0.02$) in young PLB4 mice and 1.57-fold ($p<0.0001$; $q<0.009$) in old PLB4 mice. PC aa C42:2 was reduced 1.53-fold ($p<0.001$; $q<0.08$) in young PLB4 mice and 1.19-fold ($p<0.03$; $q<0.3$) in old PLB4 mice. Overall PC aa C42:1 was the most profoundly affected metabolite (Figure 3), but all 3 showed considerable potential as biomarkers with ROC AUC values ranging from 0.80 to 0.98.

Metabolites significantly altered by age in the PLB4 genotype

A total of 14 metabolites (4 acylcarnitines, 9 PCs and 1 sphingomyelin (SM)) differed between young and old PLB4 mice which were did not differ between young and old WT (Table 4). These shortlisted metabolites showed considerable potential as biomarkers with ROC AUC values ranging from 0.84 to 1.0. Furthermore, all these metabolites increased with advancing age which the exception of PC aa C36:0 which decreased 2.31-fold ($p=0.009$; $q<0.07$). Two of the metabolites that increased (PC ae C36:3 and PC ae C42:2; 1.35-1.40-fold; $p<0.0001$; $q<0.02$)) also increased in old PLB4 compared with WT mice.

Discussion

BACE1 has been demonstrated to be the key enzyme in amyloidosis and its subsequent pathologies, and the inhibition of this enzyme is a promising therapeutic strategy through lowering cerebral Aβ concentrations in Alzheimer's disease (Yan and Vassar, 2014). The aim of this investigation was to identify the specific brain metabolite changes resulting from neural specific overexpression of BACE1. BACE1 overexpression (achieved by knock-in of hBACE1 in the PLB4 model) leads to the development of an AD-like pathology (including elevations of oligomeric Aβ assemblies, including Aβ*56 and hexameric Aβ) and it also causes an age-dependent decline in cognitive performance (Plucinska et al., 2014). We selected mice of two different age groups. Firstly, 'young' (4-6 months old) mice where changes in pathology are minimal and changes in behaviour and cognitive function are

not overt. Secondly, 'old' (8 months) mice where the pathology is more progressed with heightened levels of inflammation (gliosis) in several brain regions (dentate gyrus, hippocampal area CA1, piriform and parietal cortices) and significant impairments in spatial learning and working memory (Plucinska et al., 2014).

The use of a targeted, quantitative and reproducible metabolomics kit makes it possible to directly compare the results with other studies where this kit has also been applied (Graham et al., 2018). Compared with our group's previous study on the metabolites disturbance of the APP/PS1 mice (Pan et al., 2016), the disturbances observed here are less widespread and less severe than observed in the APP/PS1 model. All 8 significantly altered PCs were lower in 'young' PLB4 mice. This is in stark contrast to APP/PS1 mice which showed 28 PCs are significantly higher in APP/PS1 brain at 8 months. In this study the brain levels of PC aa C40:1, C42:1 and C42:2 were all significantly lower in PLB4 mice than WT – both in young and old mice brain. The PC aa 40:1 is also altered in APP/PS1 mice. In contrast, this PC is higher in 8 month old APP/PS1 mice, and not affected at 6, 10, 12 or 18 months (Pan et al., 2016). Furthermore, there are two PCs, PC ae 32:1 and PC ae 42:2, showing elevation in both 'old' PLB4 mice and APP/PS1 mice at 8 months. In PLB4 mice elevations of PC ae 42:2 were age-dependent and were not observed in the WT. The APP/PS1 transgenic mouse model expresses both mutated APP and PS1 genes which leads to an overproduction of full-length APP and monomeric Aβ. Contrastingly, PLB4 mice have pronounced expression of oligomeric Aβ species (12-meric *56, 6-mer, 4-mer, and 3-mer). Furthermore, APP/PS1 mice develop Aβ plaques as early as 5-6 months of age (Volianskis et al., 2010), whereas mature and aggregated Aβ plaques are sparse in PLB4 mice even by 12 months of age (Plucinska et al., 2014). However, both APP/PS1 and PLB4 mice show cognitive deficits at 6 months old, although the cognitive deficits in PLB4 mice may not result from Aβ plaque deposition (Plucinska et al., 2014; Xiong et al., 2011).

It is evident that the differing Aβ species present in APP/PS1 and PLB4 can result in different metabolite responses. For example, a polyamine molecule was the most significantly altered

metabolite in the present study ($p=8x10^{-8}$; $q=1x10^{-5}$). Putrescine is the precursor of other polyamines including spermine and spermidine, all of which have previously been associated with AD (Inoue et al., 2013; Trushina et al., 2013). Here, putrescine was reduced 1.31-fold in 'old' PLB4 brain and impressively generated a ROC AUC of 1.0 – marking it as a highly discriminating metabolite between PLB4 and WT littermates. However, in APP/PS1 mice putrescine is not reduced but raised, not only in brain but also in plasma (Pan et al., 2016). It has been demonstrated that intracerebroventricular infusion of pre-aggregated $A\beta_{25–35}$ significantly decreases putrescine levels the prefrontal cortex of rats (Bergin et al., 2015). Contrastingly, $A\beta_{1–41}$ upregulates of polyamine uptake and increases ornithine decarboxylase activity, which leads to increased polyamine levels in cultured neurons (Yatin et al., 2001). Therefore, the differing levels of oligomer Aβ species of the PLB4 and APP/PS1 models may explain the deviating polyamine response.

Glycerophospholipids and sphingolipids contribute to lipid bilayer asymmetry (Farooqui et al., 2010). It has been demonstrated both APP and APP-cleaving secretases are transmembrane proteins and even the cleavage of CTFα and CTFβ by γ-secretase mainly take place in lipid rafts resulting in the secretion of Aβ (Ehehalt et al., 2003; Walter and van Echten-Deckert, 2013). Furthermore, glycerophospholipids are also precursors of signalling molecules (diacylclycerol), inflammatory molecules and neurotransmitters (choline). LPCs are the hydrolysis products of PCs by Phospholipases A2 (PLA2). PLA2 enzymes have been demonstrated to directly correlate to AD pathology, not only because the PLA2 involve in the changing membrane physical properties (such as permeability and fluidity), resulting in the disturbance of Aβ production and aggregation (Evangelisti et al., 2014); but also some byproducts of PLA2 hydrolysis act as second messenger and metabolites that contribute to neuroinflammation and propagation of neuronal injury (Ong et al., 2015).

PC is the major subclass of glycerophospholipid, which is the component of biological membranes and also involved in intraneuronal signal transduction (Bazan, 2005; Yadav and Tiwari, 2014). In 'young' PLB4 mice the brain PCs which were significantly altered were of both main types (diacyl and acyl-

alkyl), and in all cases these were lower in concentration compared with WT. However, in 'old' PLB4 mice, only the diacyl PCs which were lower than the WT mice, whereas acyl-alkyl PCs are all higher in concentration. Additionally, all affected lysoPCs were higher in 'old' PLB4 mice than WT. The alteration of diacyl-PCs and acyl-alkyl PCs have been widely reported in AD patients and AD transgenic animal models (Fabelo et al., 2012; Fonteh et al., 2013; Grimm et al., 2011; Kosicek and Hecimovic, 2013; Naudi et al., 2015). Nonetheless these observations have frequently been inconsistent and inter-study variability is common. This may arise in part due to technical and methodological factors, but also it may reflect the transient metabolic responses which likely occur in a phased manner and are dependent on the actual extent of the neurodegeneration (Pan et al., 2016).

We also examined whether phospholipids disturbances observed here in female mice were consistent with those reported previously in male PLB4 mice (Plucinska et al., 2014). Lower brain levels of PC ae C30:0 (previously referred to as PC(O-30:0)) occurred in both male and female PLB4 mice of similar age. A further four lysoPCs were consistently affected in both male and female PLB4 mice. These were: lysoPC a C 16:0 (PC 16:0), lysoPC a C 18:1 (PC18:1), PC ae C34:1 (PC (O-34:1)) and PC ae C42:2 (PC (O-42:2)). Interestingly, PC ae C42:2 also elevated in the APP/PS1 mouse brain at 8 old month's age (Pan et al., 2016). It should be noted that a large number of phospholipid changes were not reproduced and diverging metabolic responses, based on gender, have the potential to confound findings in metabolomic studies unless accounted for (Krumsiek et al., 2015).

In this study, only one sphingomyelin molecule was affected. Brain levels of SM(OH)C22:2 were higher in 'old' PLB4 mice. This same sphingomyelin molecule was also elevated in the brain of 8 month old APP/PS1 mice (Pan et al., 2016). Sphingomyelin is a type of sphingolipid derived from ceramide. Most studies consistently find elevated ceramide levels in human AD brain (Bandaru et al., 2009; Filippov et al., 2012; Han et al., 2002; He et al., 2010). This may be due an upregulation of enzymes involved in sphingomyelin/ceramide metabolism during AD pathology (He et al., 2010; Panchal et al., 2014). Ceramide has also been demonstrated to stabilize BACE1 and promote the Aβ biogenesis (Patil

et al., 2007; Puglielli et al., 2003). In contrast, sphingomyelin levels in human AD brain were reported to be either increased (Bandaru et al., 2009; Pettegrew et al., 2001) or decreased (Cutler et al., 2004; He et al., 2010) depending on the brain region examined and the extent of the neuropathology.

Conclusion

This study uncovered several brain metabolite alternations occurring in female PLB4 mice with knockin of human BACE1. The majority of these metabolites increased with advancing age. Based on data in the literature we can deduce that certain metabolites are commonly affected in both in male and female PLB4 mice, however, gender-specific responses are also evident. This underlines the importance of conducting gender-specific metabolomic investigations in animal models. Furthermore, the kit-based nature of the approach used here made it possible to directly compare changes in PLB4 mice (where Aβ oligomers predominate) with other AD models such as APP/PS1 (where Aβ plaques predominate). This demonstrated that each model affected the brain metabolome differently. The divergent response of putrescine was a very notable example of this, perhaps indicating a differential effect on brain levels of ornithine decarboxylase activity. In general though the brain metabolism of PLB4 mice was much less disturbed than that of APP/PS1.

Several phospholipids are consistently affected in both of the above models and these may reflect a common, more generalised response to upregulated Aβ production in the brain. The need to pathologically stratify AD cases is becoming clearer in post-mortem human studies. Therefore, it now seems timely that systematic, longitudinal and controlled metabolomic studies are undertaken across a range of well characterised models. This will enable us to unpick the differing downstream effects of Aβ pathologies on brain metabolism.

Acknowledgement

We gratefully acknowledge Prof Bettina Platt at the School of Medicine, University of Aberdeen for the provision of mouse tissues used in these studies. Studies applying metabolomics to Alzheimer's disease have been supported by grants from Alzheimer's Research UK [ARUK-NCH2012B-5; grant ARUK-PPG2011B-8, ARUK-Network2012-11 and ARUK-Network2014-16], and a by Proof of Concept grant from Invest Northern Ireland [INI-PoC406]. We also gratefully acknowledge assistance from the European Regional Development Fund (ERDF) supporting the Advanced ASSET Centre.

Disclosure statement

The authors have no conflicts of interest to disclose.

References

Bandaru VVR, Troncoso J, Wheeler D, Pletnikova O, Wang J, Conant K, Haughey NJ. ApoE4 disrupts sterol and sphingolipid metabolism in Alzheimer's but not normal brain. Neurobiol Aging 2009;30:591-599.

Bazan NG. Lipid signaling in neural plasticity, brain repair, and neuroprotection. Mol Neurobiol 2005;32:89-103.

Bergin DH, Jing Y, Zhang H, Liu P. A single intracerebroventricular Aβ25–35 infusion leads to prolonged alterations in arginine metabolism in the rat hippocampus and prefrontal cortex. Neuroscience 2015;298:367-379.

Blennow K, de Leon MJ, Zetterberg H. Alzheimer's disease. Lancet 2006;368:387-403.

Cutler RG, Kelly J, Storie K, Pedersen WA, Tammara A, Hatanpaa K, Troncoso JC, Mattson MP. Involvement of oxidative stress-induced abnormalities in ceramide and cholesterol metabolism in brain aging and Alzheimer's disease. Proc Natl Acad Sci U S A 2004;101:2070-2075.

Ehehalt R, Keller P, Haass C, Thiele C, Simons K. Amyloidogenic processing of the Alzheimer beta-amyloid precursor protein depends on lipid rafts. J Cell Biol 2003;160:113-123.

Elder GA, Sosa MAG, De Gasperi R. Transgenic Mouse Models of Alzheimer's Disease. Mt Sinai J Med 2010;77:69-81.

Eriksson L, Kettaneh-Wold N, Trygg J, Wikström C, Wold S: Multi- and Megavariate Data Analysis : Part I: Basic Principles and Applications, Umetrics Inc, 2006.

Eriksson L, Trygg J, Wold S. CV-ANOVA for significance testing of PLS and OPLS (R) models. Journal of Chemometrics 2008;22:594-600.

Evangelisti E, Zampagni M, Cascella R, Becatti M, Fiorillo C, Caselli A, Bagnoli S, Nacmias B, Cecchi C. Plasma Membrane Injury Depends on Bilayer Lipid Composition in Alzheimer's Disease. Journal of Alzheimers Disease 2014;41:289-300.

Fabelo N, Martin V, Marin R, Santpere G, Aso E, Ferrer I, Diaz M. Evidence for premature lipid raft aging in APP/PS1 double transgenic mice, a model of Familial Alzheimer Disease. J Neuropathol Exp Neurol 2012;71:868-881.

Farooqui AA, Ong WY, Farooqui T. Lipid mediators in the nucleus: Their potential contribution to Alzheimer's disease. Biochimica Et Biophysica Acta-Molecular and Cell Biology of Lipids 2010;1801:906-916.

Filippov V, Song MA, Zhang KL, Vinters HV, Tung S, Kirsch WM, Yang J, Duerksen-Hughes PJ. Increased Ceramide in Brains with Alzheimer's and Other Neurodegenerative Diseases. Journal of Alzheimers Disease 2012;29:537-547.

Fonteh AN, Chiang JR, Cipolla M, Hale J, Diallo F, Chirino A, Arakaki X, Harrington MG. Alterations in cerebrospinal fluid glycerophospholipids and phospholipase A(2) activity in Alzheimer's disease. J Lipid Res 2013;54:2884-2897.

Graham SF, Pan X, Yilmaz A, Macias S, Robinson A, Mann D, Green BD. Targeted biochemical profiling of brain from Huntington's disease patients reveals novel metabolic pathways of interest. Biochimica et Biophysica Acta (BBA) - Molecular Basis of Disease 2018;1864:2430-2437.

Grimm MOW, Groesgen S, Riemenschneider M, Tanila H, Grimm HS, Hartmann T. From brain to food: Analysis of phosphatidylcholins, lyso-phosphatidylcholins and phosphatidylcholin

plasmalogens derivates in Alzheimer's disease human post mortem brains and mice model via mass spectrometry. J Chromatogr A 2011;1218:7713-7722.

Han XL, Holtzman DM, McKeel DW, Kelley J, Morris JC. Substantial sulfatide deficiency and ceramide elevation in very early Alzheimer's disease: potential role in disease pathogenesis. J Neurochem 2002;82:809-818.

He XX, Huang Y, Li B, Gong CX, Schuchman EH. Deregulation of sphingolipid metabolism in Alzheimer's disease. Neurobiol Aging 2010;31:398-408.

Inoue K, Tsutsui H, Akatsu H, Hashizume Y, Matsukawa N, Yamamoto T, Toyo'oka T. Metabolic profiling of Alzheimer's disease brains. Sci Rep 2013;3.

Kosicek M, Hecimovic S. Phospholipids and Alzheimer's Disease: Alterations, Mechanisms and Potential Biomarkers. Int J Mol Sci 2013;14:1310-1322.

Laird FM, Cai HB, Savonenko AV, Farah MH, He KW, Melnikova T, Wen HJ, Chiang HC, Xu GL, Koliatsos VE, Borchelt DR, Price DL, Lee HK, Wong PC. BACE1, a major determinant of selective vulnerability of the brain to amyloid-beta amyloidogenesis, is essential for cognitive, emotional, and synaptic functions. J Neurosci 2005;25:11693-11709.

Meakin PJ, Harper AJ, Hamilton DL, Gallagher J, McNeilly AD, Burgess LA, Vaanholt LM, Bannon KA, Latcham J, Hussain I, Speakman JR, Howlett DR, Ashford MLJ. Reduction in BACE1 decreases body weight, protects against diet-induced obesity and enhances insulin sensitivity in mice. Biochem J 2012;441:285-296.

Naudi A, Cabre R, Jove M, Ayala V, Gonzalo H, Portero-Otin M, Ferrer I, Pamplona R: Lipidomics of Human Brain Aging and Alzheimer's Disease Pathology; in Hurley MJ (ed): Omic Studies of Neurodegenerative Disease, Pt B. International Review of Neurobiology. 2015, vol 122, pp 133-189.

Nkuipou-Kenfack E, Duranton F, Gayrard N, Argiles A, Lundin U, Weinberger KM, Dakna M, Delles C, Mullen W, Husi H, Klein J, Koeck T, Zuerbig P, Mischak H. Assessment of metabolomic and

proteomic biomarkers in detection and prognosis of progression of renal function in chronic kidney disease. PLoS One 2014;9.

Ohno M, Cole SL, Yasvoina M, Zhao J, Citron M, Berry R, Disterhoft JF, Vassar R. BACE1 gene deletion prevents neuron loss and memory deficits in 5XFAD APP/PS1 transgenic mice. Neurobiol Dis 2007;26:134-145.

Ong WY, Farooqui T, Kokotos G, Farooqui AA. Synthetic and Natural Inhibitors of Phospholipases A(2): Their Importance for Understanding and Treatment of Neurological Disorders. ACS Chem Neurosci 2015;6:814-831.

Pan X, Bin Nasaruddin M, Elliott CT, McGuinness B, Passmore AP, Kehoe PG, Hoelscher C, McClean PL, Graham SF, Green BD. Alzheimer's disease-like pathology has transient effects on the brain and blood metabolome. Neurobiol Aging 2016;38:151-163.

Panchal M, Gaudin M, Lazar AN, Salvati E, Rivals I, Ayciriex S, Dauphinot L, Dargere D, Auzeil N, Masserini M, Laprevote O, Duyckaerts C. Ceramides and sphingomyelinases in senile plaques. Neurobiol Dis 2014;65:193-201.

Patil S, Melrose J, Chan C. Involvement of astroglial ceramide in palmitic acid-induced Alzheimer-like changes in primary neurons. Eur J Neurosci 2007;26:2131-2141.

Pettegrew JW, Panchalingam K, Hamilton RL, McClure RJ. Brain membrane phospholipid alterations in Alzheimer's disease. Neurochem Res 2001;26:771-782.

Plucinska K, Crouch B, Koss D, Robinson L, Siebrecht M, Riedel G, Platt B. Knock-In of Human BACE1 Cleaves Murine APP and Reiterates Alzheimer-like Phenotypes. J Neurosci 2014;34:10710-10728.

Plucinska K, Dekeryte R, Koss D, Shearer K, Mody N, Whitfield PD, Doherty MK, Mingarelli M, Welch A, Riedel G, Delibegovic M, Platt B. Neuronal human BACE1 knockin induces systemic diabetes in mice. Diabetologia 2016;59:1513-1523.

Prince M, Albanese E, Guerchet M, Prina M: World Alzheimer Report 2014. London, Alzheimer's Disease International, 2014.

Puglielli L, Ellis BC, Saunders AJ, Kovacs DM. Ceramide stabilizes beta-site amyloid precursor protein-cleaving enzyme 1 and promotes amyloid beta-peptide biogenesis. J Biol Chem 2003;278:19777-19783.

Roemisch-Margl W, Prehn C, Bogumil R, Roehring C, Suhre K, Adamski J. Procedure for tissue sample preparation and metabolite extraction for high-throughput targeted metabolomics. Metabolomics 2012;8:133-142.

Selkoe DJ. Alzheimer's disease: Genes, proteins, and therapy. Physiol Rev 2001;81:741-766.

Selkoe DJ. Cell biology of protein misfolding: The examples of Alzheimer's and Parkinson's diseases. Nat Cell Biol 2004;6:1054-1061.

Skovronsky DM, Lee VMY, Trojanowskiz JQ: Neurodegenerative diseases: New concepts of pathogenesis and their therapeutic implications; in: Annual Review of Pathology-Mechanisms of Disease. Annual Review of Pathology-Mechanisms of Disease. 2006, vol 1, pp 151-170.

Trushina E, Dutta T, Persson X-MT, Mielke MM, Petersen RC. Identification of altered metabolic pathways in plasma and CSF in Mild Cognitive Impairment and Alzheimer's disease using metabolomics. PLoS One 2013;8.

Volianskis A, Kostner R, Molgaard M, Hass S, Jensen MS. Episodic memory deficits are not related to altered glutamatergic synaptic transmission and plasticity in the CA1 hippocampus of the APPswe/PS1 Delta E9-deleted transgenic mice model of beta-amyloidosis. Neurobiol Aging 2010;31:1173-1187.

Walter J, van Echten-Deckert G. Cross-talk of membrane lipids and Alzheimer-related proteins. Mol Neurodegener 2013;8.

Xia JG, Sinelnikov IV, Han B, Wishart DS. MetaboAnalyst 3.0-making metabolomics more meaningful. Nucleic Acids Res 2015;43:W251-W257.

Xiong H, Callaghan D, Wodzinska J, Xu J, Premyslova M, Liu Q-Y, Connelly J, Zhang W. Biochemical and behavioral characterization of the double transgenic mouse model (APPswe/PS1dE9) of Alzheimer's disease. Neurosci Bull 2011;27:221-232.

Yadav RS, Tiwari NK. Lipid Integration in Neurodegeneration: An Overview of Alzheimer's Disease. Mol Neurobiol 2014;50:168-176.

Yan RQ, Vassar R. Targeting the beta secretase BACE1 for Alzheimer's disease therapy. Lancet Neurol 2014;13:319-329.

Yatin SM, Yatin M, Varadarajan S, Ain KB, Butterfield DA. Role of spermine in amyloid beta-peptide-associated free radical-induced neurotoxicity. J Neurosci Res 2001;63:395-401.

Table 1: Brain metabolites altered in 'young' PLB4 mice

	Metabolite	↑/↓	Fold-change	p-value	q-value	ROC (AUC)
1	Carnosine	↓	1.29	0.005847	0.21401	0.875
2	PC aa C30:0	↓	1.39	0.003618	0.16550	0.911
3	PC aa C34:4	↓	1.32	0.014078	0.42936	0.857
4	PC aa C40:1	↓	1.46	0.000660	0.06042	0.910
5	PC aa C40:2	↓	1.19	0.044784	0.79793	0.803
6	PC aa C42:1	↓	1.86	0.000097	0.01766	0.964
7	PC aa C42:2	↓	1.53	0.001297	0.07912	0.946
8	PC ae C30:0	↓	1.23	0.025710	0.67213	0.821
9	PC ae C42:1	↓	1.21	0.045724	0.79793	0.768

PC-phosphatidylcholine; aa- diacyl; ae-acyl-alkyl.

Table 2: Brain metabolites altered in 'old' PLB4 mice

	Metabolite	↑/↓	Fold-change	p-value	q-value	ROC (AUC)
1	Leucine	↑	1.23	0.039570	0.36206	0.734
2	Creatinine	↑	1.34	0.007248	0.18642	0.897
3	Putrescine	↓	1.31	0.00000008	0.00001	1.000
4	C0-AC	↑	1.19	0.010260	0.18642	0.908
5	C12-DC	↓	1.36	0.008990	0.18642	0.918
6	C14-AC	↑	1.24	0.010711	0.18642	0.857
7	C16-AC	↑	1.27	0.005925	0.18642	0.918
8	C5-OH (C3-DC-M)	↑	1.37	0.036881	0.35522	0.816
9	lysoPC a C16:0	↑	1.21	0.013243	0.18642	0.857
10	lysoPC a C18:0	↑	1.08	0.005597	0.18642	0.918
11	lysoPC a C18:1	↑	1.23	0.024669	0.30097	0.857
12	lysoPC a C20:3	↑	1.22	0.021810	0.28509	0.897
13	lysoPC a C20:4	↑	1.22	0.013203	0.18642	0.857
14	PC aa C40:1	↓	1.19	0.034570	0.35146	0.816
15	PC aa C42:1	↓	1.57	0.000095	0.00878	0.979
16	PC aa C42:2	↓	1.19	0.027634	0.31607	0.836
17	PC ae C32:1	↑	1.19	0.010114	0.18642	0.918
18	PC ae C34:1	↑	1.12	0.033835	0.35146	0.836
19	PC ae C36:3	↑	1.11	0.011563	0.18642	0.918
20	PC ae C42:2	↑	1.22	0.046399	0.40433	0.816
21	SM (OH) C22:2	↑	1.42	0.006474	0.18642	0.897

AC-acylcarnitine, DC-dioylcarnitine; lysoPC-lysophosphatidylcholine; PC-phosphatidylcholine; SM-sphingomyelin; a-acyl ; aa- diacyl; ae- acyl-alkyl.

Table 3 – Highest Ranking metabolites from Variable Importance Projection (VIP) plots for 'young' and 'old' mice. Metabolites are listed in order of their importance in the model.

A. 'young mice'			**B. 'old' mice**		
Var ID (Primary)	**M4.VIP[1]**	**1.89456 * M4.VIP[1]cvSE**	**Var ID (Primary)**	**M5.VIP[1]**	**1.89456 * M5.VIP[1]cvSE**
PC aa C42:1	3.86693	0.873218	PC aa C42:1	2.83949	1.94445
PC aa C42:2	3.01688	1.30194	SM C26:1	2.39372	2.79335
PC aa C40:1	2.8872	0.85695	Putrescine	2.3367	0.524129
SM C20:2	2.65764	3.18491	SM (OH) C22:2	2.27157	1.14677
PC aa C30:0	2.58203	1.0028	C12-DC	2.11689	1.4664
SM (OH) C24:1	2.32894	3.05933	Creatinine	2.04104	0.960955
PC aa C34:4	2.25864	1.24086	SM C20:2	1.99892	2.75372
Carnosine	2.24662	1.23569	C5-AC	1.97399	0.997821
C3-OH-AC	2.07247	2.17419	C4:1-AC	1.8981	1.71474
Histamine	1.94128	3.35882	C5-OH-AC (C3-DC-M)	1.86448	1.42254
PC ae C30:0	1.89953	0.922159	C16-AC	1.86445	1.00371
C16-OH-AC	1.88638	1.6346	C18:1-OH-AC	1.7547	1.41658
lysoPC a C26:1	1.86163	1.95737	C14-AC	1.75462	1.26952
lysoPC a C24:0	1.8341	1.21027	lysoPC a C18:0	1.73691	0.625649
PC aa C36:6	1.81703	0.677252	lysoPC a C20:3	1.64207	0.462891

AC-acylcarnitine, DC-dioylcarnitine; lysoPC-lysophosphatidylcholine; PC-phosphatidylcholine; SM-sphingomyelin; a-acyl ; aa- diacyl; ae- acyl-alkyl.

Table 4: Metabolites significantly altered with age in PLB4 which were not altered in WT mice.

	Metabolite	↑/↓	Fold-change	p-value	q-value	ROC (AUC)
1	PC ae C36:3	↑	1.35	5.95E-05	0.002677	1
2	PC ae C34:2	↑	1.35	7.02E-04	0.014047	0.94
3	PC ae C42:2	↑	1.40	0.001655	0.024887	0.98
4	C18:1-OH-AC	↑	1.67	0.003957	0.046937	0.90
5	PC ae C38:1	↑	1.31	0.004501	0.046937	0.90
6	PC ae C40:2	↑	1.37	0.004694	0.046937	0.90
7	C3-OH-AC	↑	1.52	0.005984	0.056691	0.90
8	PC ae C42:1	↑	1.28	0.006933	0.062394	0.88
9	SM (OH) C22:1	↑	1.91	0.008095	0.065566	0.88
10	PC aa C36:0	↓	2.31	0.009474	0.06821	0.88
11	C16-AC	↑	1.24	0.01815	0.1252	0.88
12	PC aa C38:0	↑	1.19	0.01878	0.1252	0.84
13	C14-AC	↑	1.21	0.024135	0.15516	0.88
14	PC ae C44:4	↑	1.26	0.044972	0.25351	0.84

Values were obtained by comparing 'young' and 'old' PLB4 mice and by cross-referencing against an identical comparison in WT mice. AC-acylcarnitine, PC-phosphatidylcholine; SM-sphingomyelin; aa-diacyl; ae- acyl-alkyl.

Figure Legends

Figure 1. Multivariate statistical models arising from targeted metabolomics data. (A) Unsupervised PCA scores plot (R^2≤0.537; Q^2≤0.311)and (B) OPLS-DA scores plot (R^2≤0.69; Q^2≤0.51) classifying brain samples from young WT (open circles), young PLB4 (closed circles), old WT (open triangles) and old PLB4 (closed triangles) mice. Data were normalised by log-transform and pareto-scaled. (C) Permutation plot (n = 999) for the OPLS-DA model built for brain samples from young WT, young PLB4, old WT and old PLB4 mice (R2 = green circles, Q2 = blue squares).

Figure 2. Heat-map of top 10 affected metabolites in female PLB4 mice. Data were normalised by log-transform and pareto-scaled and heat maps were created using Metaboanalyst (Distance Measure: Euclidean). The top 10 metabolites affected (as selected by t-test p-value) were shortlisted for (A) young and (B) old mice.

Figure 3. Concentrations of PC aa C42:1 significantly differ in both young and old PLB4 mice. Three brain PCs were commonly affected in both young and old PLB4 mice, of these PC aa C42:1 was the most profoundly affected. Figures show the brain concentrations of PC aa C42:1 in (A) young mice (B) old mice presented as box and whisker plots (n=7-8). (C) Receiving operator characteristic (ROC) curves constructed individually for young (open circles; WT vs PLB4) and old (open triangles; WT vs PLB4). Figures were produced using GraphPad Prism (version 6.03).

Figure 1

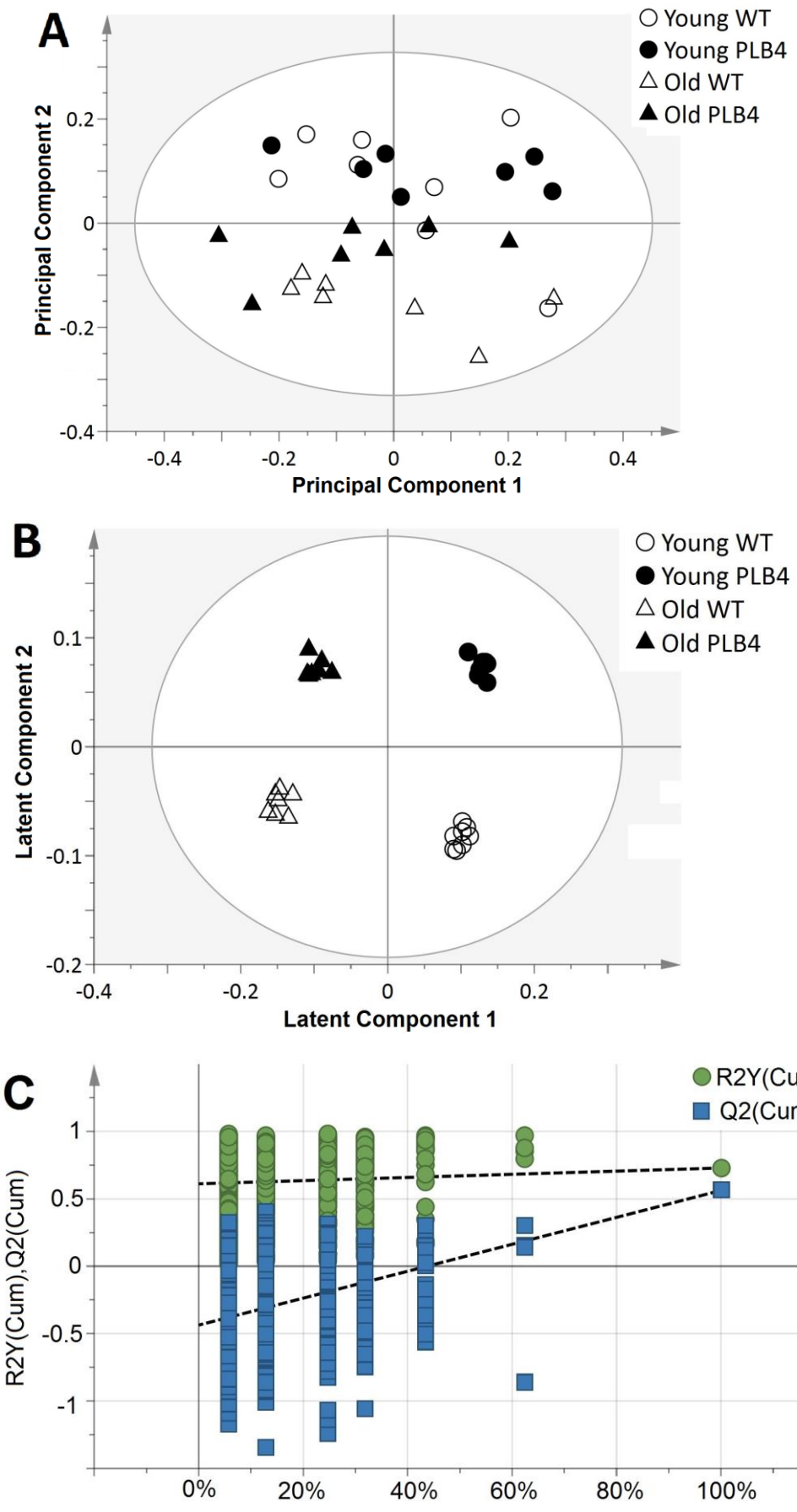
A
Young WT
Young PLB4
Old WT
Old PLB4
Principal Component 2
Principal Component 1
0.2
0
-0.2
-0.4
-0.4
-0.2
0
0.2
0.4
B
Young WT
Young PLB4
Old WT
Old PLB4
Latent Component 2
Latent Component 1
0.1
0
-0.1
-0.2
-0.4
-0.2
0
0.2
C
R2Y(Cum)
Q2(Cum)
R2Y(Cum),Q2(Cum)
1
0.5
0
-0.5
-1
0%
20%
40%
60%
80%
100%

Figure 2

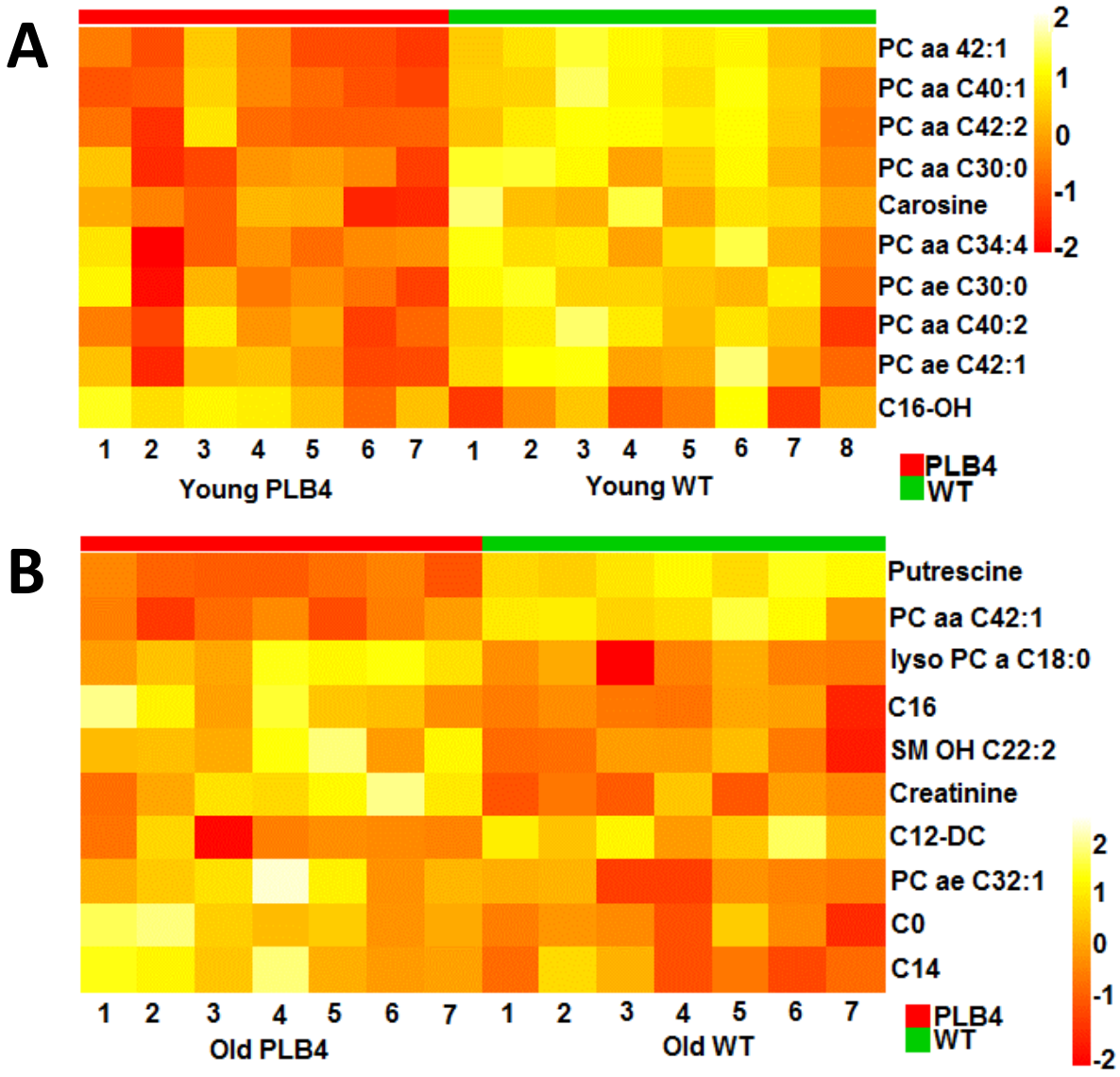
A
PC aa 42:1
PC aa C40:1
PC aa C42:2
PC aa C30:0
Carosine
PC aa C34:4
PC ae C30:0
PC aa C40:2
PC ae C42:1
C16-OH
2
1
0
-1
-2
1 2 3 4 5 6 7 1 2 3 4 5 6 7 8
Young PLB4
Young WT
PLB4
WT
B
Putrescine
PC aa C42:1
lyso PC a C18:0
C16
SM OH C22:2
Creatinine
C12-DC
PC ae C32:1
C0
C14
2
1
0
-1
-2
1 2 3 4 5 6 7 1 2 3 4 5 6 7
Old PLB4
Old WT
PLB4
WT

Figure 3

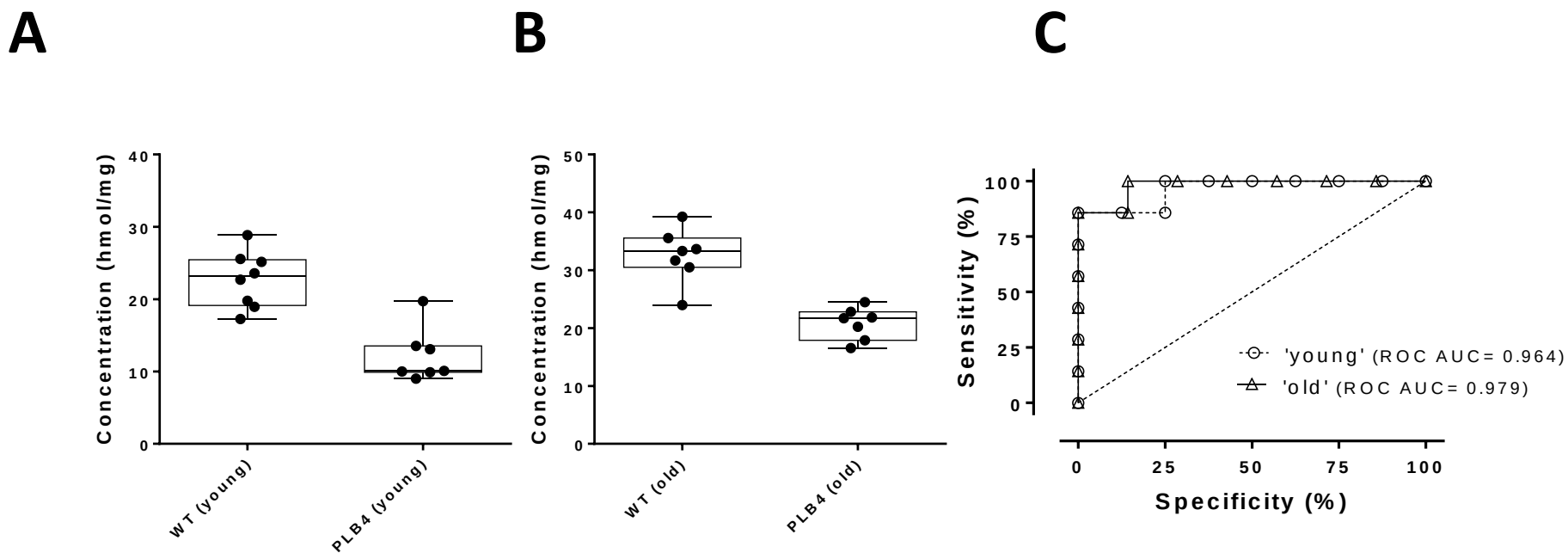
A
B
C
Concentration (hmol/mg)
40
30
20
10
0
WT (young)
PLB4 (young)
Concentration (hmol/mg)
50
40
30
20
10
0
WT (old)
PLB4 (old)
Sensitivity (%)
100
75
50
25
0
0
25
50
75
100
Specificity (%)
'young' (ROC AUC= 0.964)
'old' (ROC AUC= 0.979)